The diffusion-induced nova scenario: CK Vul and PB8 as possible observational counterparts

M. M. Miller Bertolami,[1,2]★ L. G. Althaus,[1,2] C. Olano[1] and N. Jiménez[1,2]

[1]*Facultad de Ciencias Astronómicas y Geofísicas, Univ. Nac. de La Plata, Paseo del Bosque s/n, La Plata, Argentina*
[2]*Instituto de Astrofísica La Plata, UNLP-CONICET, Paseo del Bosque s/n, La Plata, Argentina*

ABSTRACT

We propose a scenario for the formation of DA white dwarfs with very thin helium buffers. For these stars we explore the possible occurrence of diffusion-induced CNO-flashes during their early cooling stage. In order to obtain very thin helium buffers, we simulate the formation of low-mass remnants through an asymptotic giant branch (AGB) final/late thermal pulse (AFTP/LTP scenario). Then we calculate the consequent white dwarf cooling evolution by means of a consistent treatment of element diffusion and nuclear burning.

Based on physically sound white dwarf models, we find that the range of helium buffer masses for these diffusion-induced novae to occur is significantly smaller than that predicted by the only previous study of this scenario. As a matter of fact, we find that these flashes do occur only in some low-mass ($M \lesssim 0.6\,\mathrm{M_\odot}$) and low-metallicity ($Z_{\mathrm{ZAMS}} \lesssim 0.001$) remnants about 10^6–10^7 yr after departing from the AGB. For these objects, we expect the luminosity to increase by about 4 orders of magnitude in less than a decade. We also show that diffusion-induced novae should display a very typical eruption light curve, with an increase of about a few magnitudes per year before reaching a maximum of $M_V \sim -5$ to -6. Our simulations show that surface abundances after the outburst are characterized by $\log N_{\mathrm{H}}/N_{\mathrm{He}} \sim -0.15 \ldots 0.6$ and $N > C \gtrsim O$ by mass fractions. Contrary to previous speculations we show that these events are not recurrent and do not change substantially the final H-content of the cool (DA) white dwarf.

Finally, with the aid of model predictions we discuss the possibility that Nova Vul 1670 (CK Vul) and the recently proposed [WN/WC]-central stars of planetary nebulae could be observational counterparts of this diffusion-induced nova scenario. We conclude that, despite discrepancies with observations, the scenario offers one of the best available explanations for CK Vul and, with minor modifications, explains the observed properties of [WN/WC]-central stars of planetary nebulae.

Key words: stars: AGB and post-AGB – stars: individual: CK Vul – stars: individual: PB8 – white dwarfs – stars: Wolf–Rayet.

1 INTRODUCTION

It is well known that element diffusion plays a major role in shaping the chemical stratification of white dwarfs (WDs; Koester & Chanmugam 1990). Gravitational settling is responsible for the chemical purity of the outer layers of WDs. Due to the very high surface gravities of these stars the lightest element remaining in the WD (either H or He) floats up and forms a pure envelope, the thickness of which gradually increases as the WD evolves. On the other hand, the large chemical gradients formed during the previous evolution lead to chemical diffusion which, in turn, will smooth out the chemical profile of cool WDs (e.g. Renedo et al. 2010). Recently, the gravitational settling of ^{22}Ne in the liquid interior of WDs has been found to be a key ingredient to explain the cooling age of the old, metal-rich, open cluster NGC 6791 (Althaus et al. 2010b; García-Berro et al. 2010).

Since the first simulations of WD evolution that included a simultaneous treatment of diffusion and cooling (i.e. Iben & MacDonald 1985, 1986, hereafter IM86), it was noticed that diffusion could trigger thermonuclear CNO-flashes. In fact, the inwards diffusion of H and the outwards diffusion of C within the pure He zone that is located below the H-rich envelope and above the C-rich intershell (usually named 'He-buffer'; see Fig. 1) can lead to a runaway
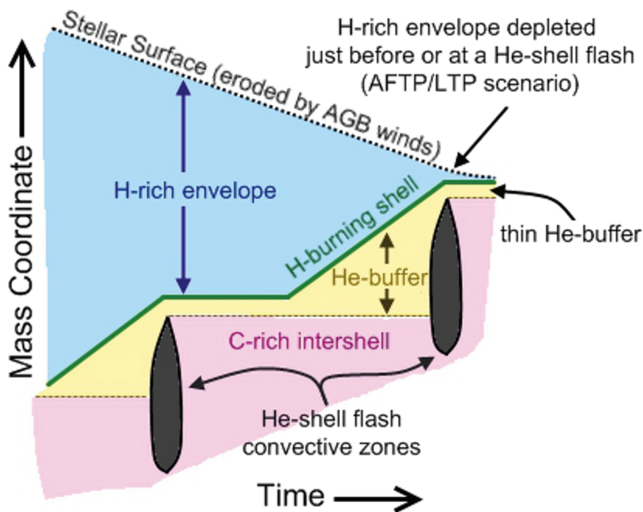
★E-mail: mmiller@fcaglp.unlp.edu.ar

Figure 1. Sketch of a Kippenhahn diagram of the proposed scenario for the formation of DA WDs with thin He-buffers.

CNO-burning. This possibility was shown by IM86 who found that, if the He-buffer was thin enough, C and H can come into contact and develop an unstable H-burning. This sudden energy release produces a very rapid expansion, of the order of years, of the outer layers of the WD pushing the star back to a giant configuration and increasing its visual magnitude from $M_V \sim 9$ to $M_V \sim -6$ in a few years. We term this eruptive event as 'diffusion-induced nova'[1] (DIN) although it leads to a much slower brightening than classical novae. IM86 showed that after such events the stars will become, in a few years, yellow giants with mildly He-enriched surface compositions. In a more speculative mood they also suggested that DINs may be recurrent, finally leading to H-deficient compositions. Later, prompted by this speculation, D'Antona & Mazzitelli (1990) suggested that the H-rich envelope could be strongly reduced during these events, leading to DA WDs with thin H-envelopes, as inferred in some DA WDs (Castanheira & Kepler 2009).

Since the first exploratory simulation performed by IM86, these DINs have been mentioned in several review papers and books (D'Antona & Mazzitelli 1990; Iben 1995; Hansen 2004; Salaris & Cassisi 2005 and more recently Althaus et al. 2010a), but no new numerical experiments have been performed. The latter becomes particularly relevant in light of the criticism made by Mazzitelli & D'Antona (1986) that the pre-WD models adopted by Iben & MacDonald (1985) and IM86 were not realistic enough. In this context, a re-examination of the possibility and characteristics of DINs is in order.

As mentioned, DINs are expected to increase their visual magnitudes from $M_V \sim 9$ to $M_V \lesssim -5$ in a few years. IM86 mentioned that such event would display a light curve similar to that of a very slow nova. The most famous object with such description is the enigmatic Nova Vul 1670 (CK Vul), the oldest catalogued nova variable (Trimble 2000). First discovered by Père Dom Anthelme on 1670 June 20, and later independently by Johannes Hevelius on July 25, CK Vul seem to have raised to 3rd magnitude in less than a year (Shara, Moffat & Webbink 1985), although no pre-maximum obser-

vations exist. Its eruption lasted for two years (1670–1672). During that period it faded and brightened two times before definitely disappearing from view. Three centuries later, Shara & Moffat (1982) partially recovered the remnant. They discovered several nebulosities that were conclusively linked to the 1670 eruption by Hajduk et al. (2007) through proper motion studies. CK Vul remains a very enigmatic object and several scenarios have been proposed to explain its observed behaviour. In fact, it has alternatively been proposed to be an hibernating nova, a very late thermal pulse (VLTP), a 'gentle' supernova, a light nova and a stellar merger event (Kato 2003; Hajduk et al. 2007). None of the proposed scenarios seems to correctly describe the observations (Hajduk et al. 2007), although the VLTP seems to be the preferred one (Harrison 1996; Evans et al. 2002 and Hajduk et al. 2007). In this context, and due to the similarities between post-VLTP evolution and post-DIN evolution, it seems worth analysing whether CK Vul could be understood within the DIN scenario.

The main purpose of the present article is to study the possibility that DINs could take place in physically sound WD models with a realistic evolutionary history. We will also identify a detailed scenario for the creation of WDs with thin enough He-buffers for DIN events to occur. Specifically, to perform this study we compute realistic WD models by means of 'cradle-to-grave' stellar evolution simulations. Then, we compute WD cooling sequences by considering a simultaneous treatment of element diffusion and evolution.

This article is organized as follows. In the next section we briefly describe the input physics adopted in the present simulations. Then, in Section 3, we identify a possible evolutionary scenario that can lead to WDs with thin He-buffers. Once the evolutionary scenario has been set we present our numerical simulations and results (Section 4). In particular, we show that the proposed scenario can effectively produce WD models with thin He-buffers. Then, we discuss the main predictions of the simulations and explore under which conditions DINs might occur. Furthermore, we make a very detailed description of the sequence of events before, during and after the DIN events. Once the predictions of DIN simulations have been clarified, in Section 5 we look for possible observational counterparts of these events. In particular, we speculate that DINs could be the origin of CK Vul and PB8 (the prototype of the recently proposed [WN/WC]-CSPNe; see Todt et al. 2010) and show that, although significant discrepancies exist, the DIN scenario offers a possible explanation for these objects. Finally, we close the article with some final statements and conclusions.

2 BRIEF DESCRIPTION OF THE STELLAR EVOLUTION CODE

The simulations presented here have been performed with the LPCODE stellar evolution code (see Renedo et al. 2010). LPCODE is a well-tested and amply used evolutionary code that is particularly appropriate to compute realistic WD structures and their evolution by means of 'cradle-to-grave' stellar evolution simulations, and allows for a consistent and detailed computation of the effects of element diffusion during the WD cooling phase. As this work is aimed at exploring the outburst properties of diffusion-induced CNO-flashes on hot WDs, it is worth mentioning that LPCODE has been previously used to study other kinds of H-flashes on (very) hot WDs. These include simulations of the post-AGB born-again scenario (Miller Bertolami & Althaus 2007), and the post-red giant branch (post-RGB) hot-flasher scenario (Miller Bertolami et al. 2008) for the formation of H-deficient WDs and subdwarfs, respectively. Numerical and physical aspects of

---

[1] IM86 named these events self-induced novae, but we will use the term 'diffusion-induced novae' to distinguish them from late helium-flashes (born-again AGB stars; Iben 1984) which predict similar light curves and can also be considered 'self-induced'.

LPCODE can be found in Althaus et al. (2005). In what follows we only comment on the physical inputs regarding the treatment of diffusion processes that are specifically relevant for the present work.

WD models are obtained as the result of computing the evolution of low-mass stars from the zero-age main sequence (ZAMS) through the helium core flash and through the thermal pulses on the AGB (TP-AGB) and, then, to the WDs stage. LPCODE considers a simultaneous treatment of non-instantaneous mixing and burning of elements by means of a diffusion picture of convection coupled to nuclear burning [see Althaus et al. (2005) for numerical procedures]. The nuclear network considered in the present work accounts explicitly for the following 16 elements: ^{1}H, ^{2}H, ^{3}He, ^{4}He, ^{7}Li, ^{7}Be, ^{12}C, ^{13}C, ^{14}N, ^{15}N, ^{16}O, ^{17}O, ^{18}O, ^{19}F, ^{20}Ne and ^{22}Ne, together with 34 thermonuclear reaction rates corresponding to the pp-chains, the CNO bi-cycle, He-burning and C-ignition as described in Miller Bertolami et al. (2006).

As mentioned in the Introduction, element diffusion strongly modifies the chemical profiles throughout the outer layers of WDs. In this work the WD evolution was computed in a consistent way with the changes of chemical abundances as a consequence of diffusion. The treatment is similar to that of Iben & MacDonald (1985) and IM86 but we consider, in addition to gravitational settling and chemical diffusion, the process of thermal diffusion. We do not take into account radiative levitation, as it is only relevant for determining surface chemical abundances and, thus, is irrelevant for the purpose of the present work. Our treatment of time-dependent element diffusion is based on the multi-component gas picture of Burgers (1969). Specifically, we solved the diffusion equations within the numerical scheme described in Althaus et al. (2003).

3 THE EVOLUTIONARY SCENARIO

The formation of a WD with a very thin He-buffer seems to be a key factor in the occurrence of a DIN episode (see IM86). IM86 obtained a pre-WD model with a thin He-buffer by abstracting mass from an AGB star model shortly after it has experienced an He-flash. Mazzitelli & D'Antona (1986) noted that the way this pre-WD model was created is artificial and could affect the thermal properties of the remnant. Whether WDs with thin He-buffer can be actually formed relies on identifying a scenario in which they could be formed under standard assumptions. As shown in Fig. 1, after an He-shell flash on the TP-AGB, the mass of the He-buffer region becomes strongly reduced by intershell convection. Such thin He-buffer survives until the re-ignition of the H-burning shell. Note that this may not be true if the star experiences third dredge up events, during which the deepening of the H-rich envelope will erase the remaining He-buffer by diluting it into the envelope. From this moment on, the He-buffer mass starts to increase until the next He-shell flash. In this context, a realistic scenario that can lead to a DA WD with a thin He-buffer can be outlined. Recent studies on the initial–final mass relation (Kalirai et al. 2008; Salaris et al. 2009) support the absence of significant third dredge up in low-mass stars (Karakas 2003). In particular, the first thermal pulses of low-mass stars ($M \lesssim 1.5\,M_{\odot}$) are not very strong and, thus, no third dredge up takes place in numerical models. Hence, it is not unreasonable to accept that low-mass stars experiencing an AGB final thermal pulse (AFTP) or a late thermal pulse (LTP) will end as DA WDs with thin He-buffers. In those cases, as no third dredge up happens, the very thin He-buffer survives the last helium shell flash (either AFTP or LTP). Then, during the He-burning phase that follows the flash, AGB winds will erode an important fraction of the remaining

(already depleted) H-rich envelope, preventing a re-ignition of the H-burning shell and an increase in the He-buffer mass. As a result, the He-buffer is still very thin when the star finally reaches the WD phase. We propose that this scenario can lead to WDs with thin He-buffers and therefore might lead to DINs.

In order to bear out the scenario described in the preceeding paragraph we have computed several sequences from the ZAMS to the TP-AGB under standard assumptions [see Renedo et al. (2010) for a description]. In particular, we have included overshooting (OV) only in core convective zones within a diffusive convective picture as in Miller Bertolami & Althaus (2006). Thus, no OV mixing has been included during the TP-AGB evolution of any sequence, as it leads to strong third dredge up episodes in low-mass AGB stars. Although the efficiency of third dredge up on AGB stars is clearly not a solved problem, it is clear that third dredge up is less efficient in low-mass stars than in the more massive stars (e.g. Karakas, Lattanzio & Pols 2002). In this connection, Salaris et al. (2009) have shown that strong third dredge up is disfavoured by the semi-empirical initial–final mass relation, for stars with masses lower than $4\,M_{\odot}$. It is worth noting that their study only deals with stars of masses $M > 2\,M_{\odot}$ and cannot be directly applied to our work. However, as third dredge up efficiency is expected to decrease for stars of lower masses, it seems safe to assume that no third dredge up should be present in stars of even lower masses. In agreement with this, Guandalini et al. (2006) have suggested that the properties of carbon stars can be explained if no OV is added in low-mass AGB stellar models. It must be noted, however, that both Salaris et al. (2009) and Guandalini et al. (2006) deal with stars of higher metallicities than studied in the present work and third dredge up is expected to increase at lower metallicities. The absence of third dredge up episodes in low-mass AGB stars is of special importance for the scenario outlined in the previous paragraph, as third dredge up erodes the thin He-buffer formed just after a thermal pulse. It is worth noting that mass-loss rates during the RGB and AGB phases have been adopted according to the prescriptions of Schröder & Cuntz (2005) and Vassiliadis & Wood (1993). This choice, together with the absence of third dredge up, is expected to produce a realistic initial–final mass relation. The only exception is mass loss just before the final helium flash, which was tuned to obtain an AFTP/LTP episode according to the scenario proposed here. It is worth mentioning that standard AGB winds have been adopted during the He-burning phase *after* the last helium flash (AFTP/LTP), when the star becomes a born-again AGB star. No mass loss has been adopted during the high-temperature ($T_{\rm eff}$) phase of pre-WD evolution.

4 RESULTS

In the previous section, we mentioned that several sequences have been calculated for the present study. As all our DIN sequences display similar characteristics, we will first describe the evolution of a chosen reference sequence. Then, we will discuss how differences in progenitor/remnant masses, initial metallicities and He-buffer thicknesses may affect the course of evolution. In particular, we will show in later sections the range in the predicted abundances and time-scales of all our computed sequences, as well as the characteristics of those sequences that did not undergo DIN episodes.

4.1 Detailed description of a reference sequence

The evolution of our reference sequence in the Hertzsprung–Russell (HR) diagram is shown in Fig. 2. It corresponds to an initially
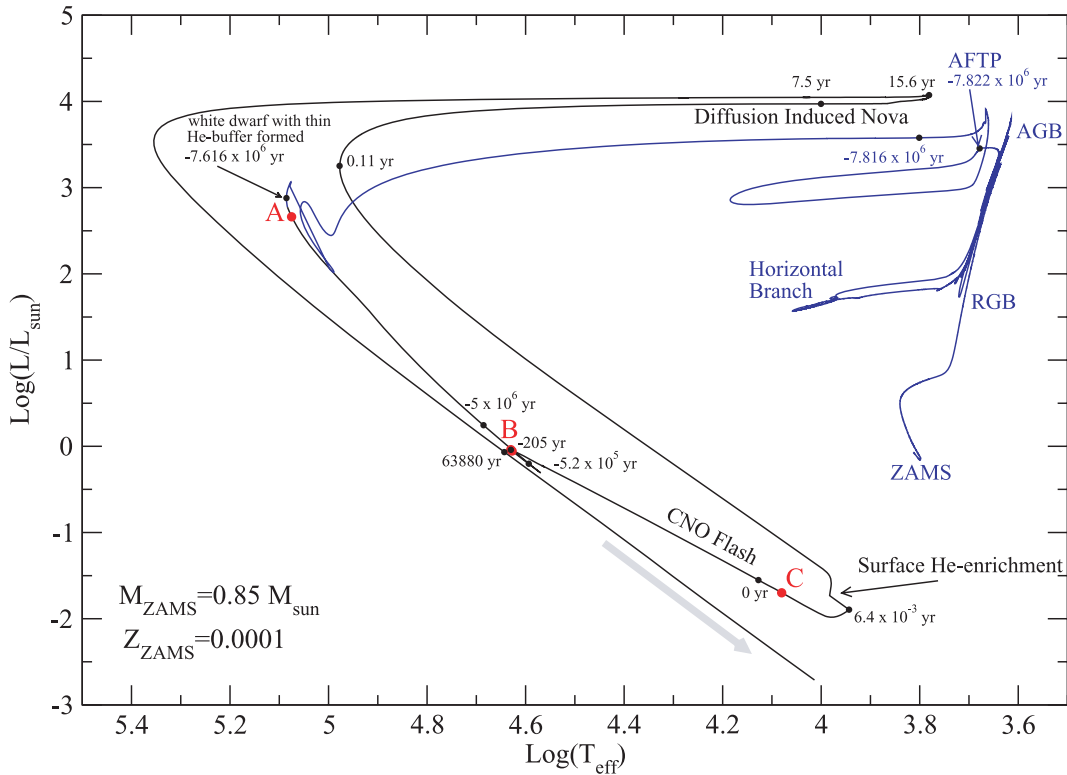
Figure 2. HR-diagram evolution of an initially $0.85\,M_\odot$ star with $Z = 1 \times 10^{-4}$. It undergoes its final thermal pulse on the AGB with a thin envelope and consequently no important H-re-ignition takes place before reaching the WD cooling stage. This produces a WD with a very thin He-buffer which experiences a DIN due to the diffusive mixing of C and H in the He-buffer (see Fig. 3). Time has been chosen to be $t = 0$ at the point of maximum energy release by H-burning during the CNO-flash.

$M = 0.85\,M_\odot$ (ZAMS) model star with $Z = 0.0001$. After evolving through the central H- and He-burning, the star starts climbing the early AGB. This is so until the development of the first thermal pulse ($t_{age} = 11\,757.6\,\mathrm{Myr}$, $M = 0.584\,M_\odot$), which marks the beginning of the TP-AGB phase. The mass of the hydrogen-free core at that point is $M_{HFC} = 0.515\,M_\odot$. Due to the low mass of the star at the beginning of the TP-AGB, and owing to the relatively high winds ($\dot{M} \sim 10^{-7}\,M_\odot\,\mathrm{yr}^{-1}$) the star suffers during the TP-AGB and the long interpulse period ($P \sim 530\,000\,\mathrm{yr}$), the star experiences only three thermal pulses. Mass loss during the very end of the TP-AGB was tuned for the last thermal pulse to develop when the star was just leaving the AGB (an AFTP). The mass at the moment of the AFTP is $M = 0.544\,03\,M_\odot$ with a hydrogen-free core mass of $M_{HFC} = 0.538\,39\,M_\odot$. After winds have reduced the mass of the star to $0.539\,46\,M_\odot$, the star leaves the AGB ($T_{eff} \gtrsim 10\,000\,\mathrm{K}$) and evolves towards the WD stage with an H-envelope of $M_{env}^{pre\text{-}WD} = 1.07 \times 10^{-3}\,M_\odot$,[2] which corresponds to a total H-content of $M_H^{pre\text{-}WD} = 6.6 \times 10^{-4}\,M_\odot$, and an He-buffer thickness of only $M_{Buffer}^{pre\text{-}WD} = 1.37 \times 10^{-4}\,M_\odot$. Before entering the WD stage H is re-ignited, this produces the kink in the HR diagram (see Fig. 2) just before the point of maximum T_{eff}. As a consequence of this re-ignition, both the mass of the H-envelope and the total H-content of the star are diminished to $8.5 \times 10^{-4}\,M_\odot$ and $4.2 \times 10^{-4}\,M_\odot$, respectively. Conversely, the mass of the He-buffer zone is increased up to $M_{Buffer} = 4.38 \times 10^{-4}\,M_\odot$. At this point the sequence begins its cooling as a WD with a thin He-buffer (see

Fig. 2). The chemical profile at that point is shown in Fig. 3 (panel A). From that point onwards, the star cools and contracts as a WD. Simultaneously, chemical profiles are altered by element diffusion. In particular, H from the envelope and C from the intershell region, just below the He-buffer (see Fig. 1), diffuse through the He-buffer due to chemical diffusion triggered by the steep chemical profiles left by the previous evolution. Fig. 3 (panel B) shows the chemical profile $7.58 \times 10^6\,\mathrm{yr}$ after the WD started its cooling evolution. At this point the amount of C and H diffused into the He-buffer and, consequently, the rate of energy generated by CNO burning start to increase. From this point onwards CNO burning increases slowly until $\log L_H/L_\odot \sim 1.5$ when the rate of energy generated by CNO burning leads to the development of convection (about $23\,000\,\mathrm{yr}$ after CNO burning started to increase). This convective zone drags H from regions with higher H mass fractions and thus leads to higher energy generation rates. As a consequence the star enters a quicker phase and in less than $200\,\mathrm{yr}$ L_H rises to $\log L_H/L_\odot \sim 7.5$. This sudden energy injection causes a very quick expansion of the layers on top of the H-burning shell and the star is ballooned back to the giant branch in a few years (see Fig. 2). In Fig. 4 we show the predicted visual light curve for the outburst episode – $t = 0$ denotes the instant of maximum energy release by the CNO-flash (panel C of Fig. 3, see also Fig. 2). Visual magnitudes have been obtained from the predicted luminosity of the sequences and adopting the bolometric corrections derived by Flower (1996) for normal H-rich abundances. As can be seen after suddenly rising from $M_V \sim 9$ to $M_V \sim 2$ the star increases its visual magnitude much slower than a classical nova, at a speed of $\sim 1\,\mathrm{mag}\,\mathrm{yr}^{-1}$. Specifically, the brightening speed just before reaching its maximum (at $M_V \sim -5.2$, $\sim 8\,\mathrm{yr}$ after the H-flash) is $dM_V/dt \sim 1.6\,\mathrm{mag}\,\mathrm{yr}$. Just after the maximum energy

---

[2] We define the H-envelope as those regions with an H-content greater than 1×10^{-4} by mass fraction.
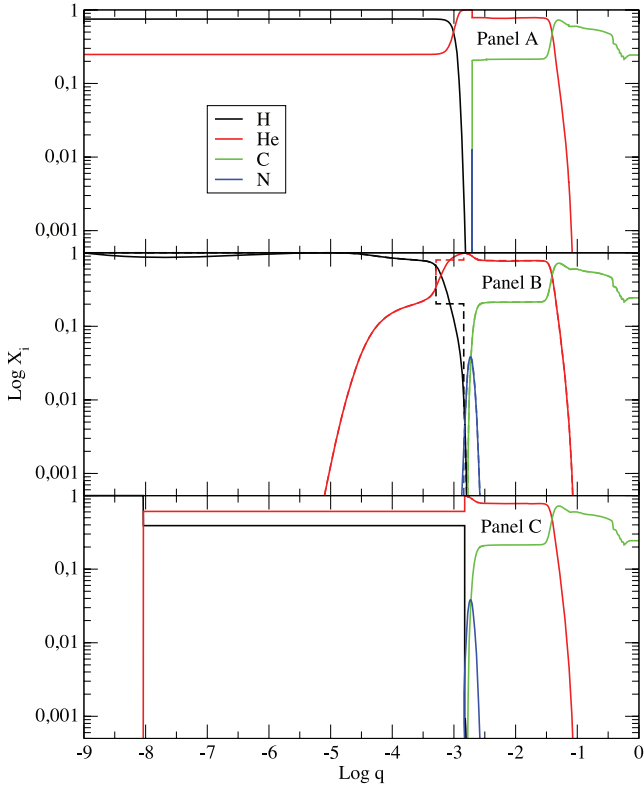
Figure 3. Evolution of the chemical profiles of our reference sequence ($0.539\,46\,M_{\odot}$). Panels A, B and C correspond to the instants denoted by the same letters in Fig. 2. Dashed lines in the middle panel indicate profiles just after the development of the convective zone driven by the H-flash.
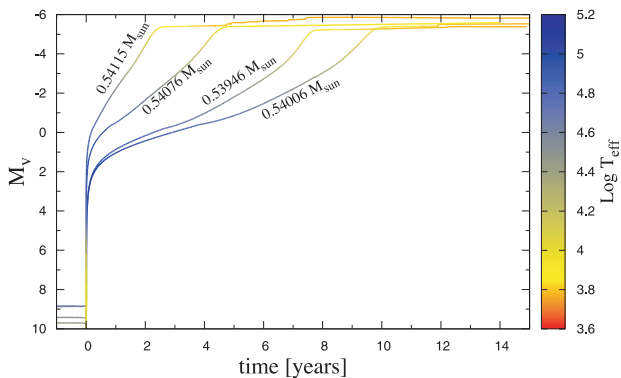

Figure 4. Predicted light curves for the DINs of remnants coming from an initially $M = 0.85\,M_{\odot}$, $Z = 0.0001$ star. Different remnant masses were obtained by altering the wind intensity during the AFTP. Visual magnitudes were obtained from the predicted luminosity of the sequences and adopting the bolometric corrections derived by Flower (1996).

release by the H-flash, when the star moves to low temperatures and luminosities, the convective region driven by the H-flash merges with the (very thin) external convective region caused by low temperature opacity. Then, the material from the very outer layers of the star is mixed with the material of the flash-driven convective region. Consequently, the surface abundances of the model are altered. The amount of He rises significantly ($X_{He} = 0.61$ by mass fraction) while the H mass fraction is reduced ($X_{H} = 0.39$). Then, the DIN gives rise to an object with a mild H-deficiency. Also N is increased at the surface of the star. As the inner regions, which have experienced
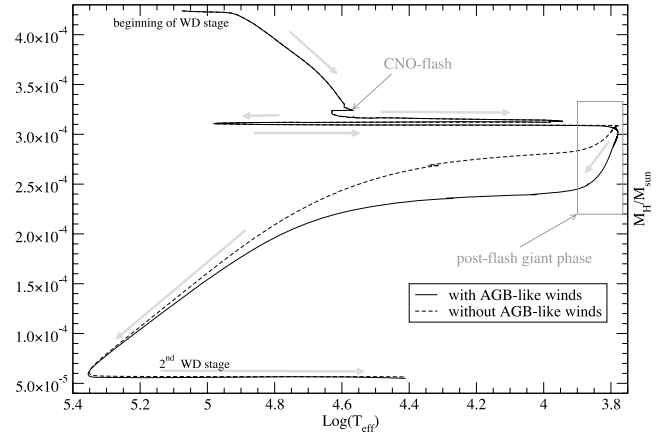

Figure 5. Evolution of the total H-content of our reference WD sequence. The solid line shows the evolution in the case that AGB-like winds are considered during the second AGB phase after the CNO-flash, while the dashed line indicates the evolution of the H-content in the case no AGB-like winds have been considered. Note that regardless of the intensity of winds in this stage the final H-content of the DA WD is not modified and is of the order of $M_{H} \sim 5 \times 10^{-5}\,M_{\odot}$.

CNO burning, are N-enhanced, the surface abundance of N during the outburst increases to 2.2×10^{-4}, significantly higher than the mass fractions of C and O (1×10^{-5} and 1.1×10^{-6}, respectively), and higher than the surface N abundance before the outburst ($N \sim 1.56 \times 10^{-5}$). Once back at low effective temperatures the star is expected to undergo strong winds similar to those of AGB stars. The time spent at low effective temperatures during this stage will be strongly dependent on mass-loss assumptions. If standard AGB mass loss is assumed, then the star reheats back to $T_{eff} \gtrsim 10\,000\,K$ in about $\sim 50\,yr$, while in the case of no significant mass loss the star stays at low effective temperature for about $\sim 260\,yr$. Under the assumption of standard AGB mass loss, the total mass lost by the object before it starts to contract again is of $1.6 \times 10^{-4}\,M_{\odot}$ (see Fig. 5). Finally, the star returns to the WD cooling track. The model returns to its pre-outburst stage ($\log L/L_{\odot} \sim -0.25$ and $\log T_{eff} \sim 4.6$) in only $\sim 10^{5}\,yr$, much faster than in its pre-outburst cooling, which took $\sim 7.6 \times 10^{6}\,yr$. This should not be a surprise as only the outer layers are affected by the eruption and, so, the interior of the WD still resembles the structure prior to the eruption (see Fig. 6). Only the outer layers, which have much shorter thermal time-scales, cool and contract during this second WD stage. The main consequence of this fast cooling is that diffusion has not enough time to alter the composition of the inner regions of our new WD at high effective temperatures and the luminosity of the CNO-burning shell remains very low. Then, no new CNO-flash does take place this second time.

4.2 Dependence on physical and numerical parameters

In order to understand to what extent the outburst properties depend on the remnant properties, we have performed several simulations under different assumptions. Specifically, we have calculated the outburst for remnants of different masses and also for remnants coming from progenitors of different masses. We also explore how thin the He-buffer needs to be in order to obtain a DIN. The latter is an important issue to understand how frequent these events might be.

To assess the importance of the He-buffer thickness for the development of DIN, we have computed four additional sequences by
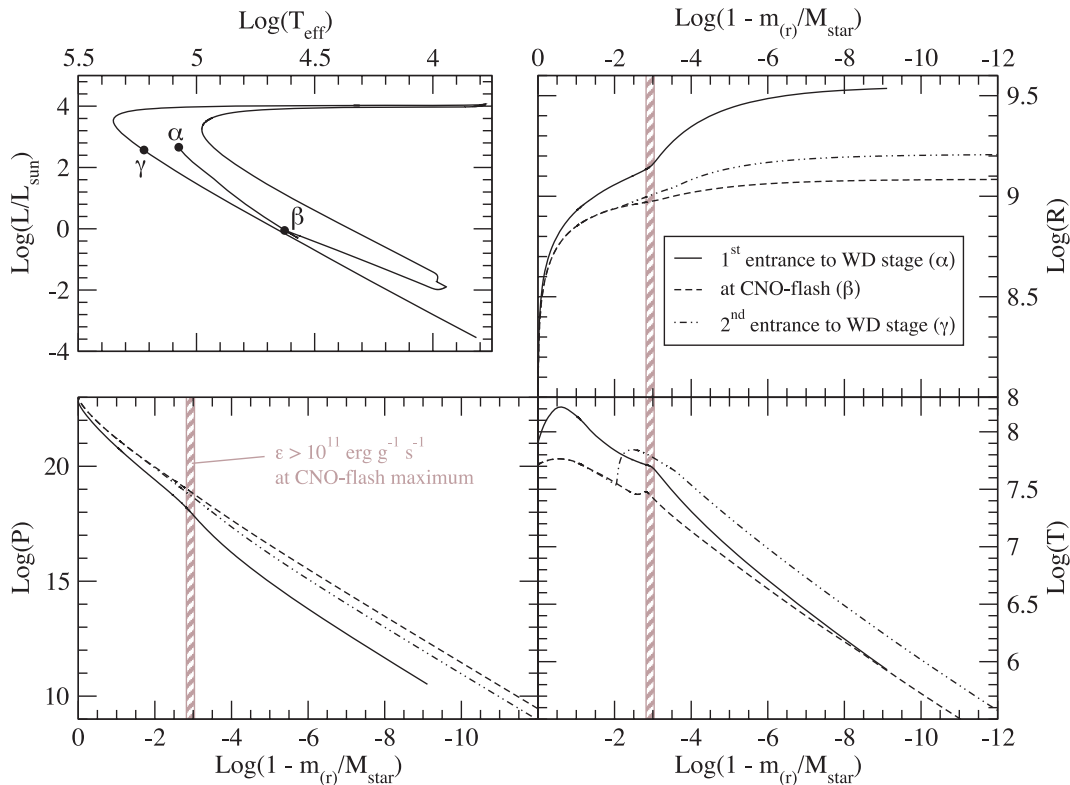
Figure 6. Structure variables [$P(m)$, $T(m)$ and $r(m)$] at three different stages (α, β and γ see the upper-left panel) of the WD evolution. Note that the interior ($\log(1 - m/M_\star) > -3$) structure of the WD just before (β) and after (γ) the flash is almost unchanged.

Table 1. Properties of post-AGB remnants of an initially $0.85\,M_\odot$ star with $Z = 1 \times 10^{-4}$ which experiences a final thermal pulse (see text for details). M_{env} is the mass of the outer layers with $X_H > 10^{-4}$. M_{Buffer} is the thickness of the almost pure He layers (He-buffer). M_H is the total hydrogen content of the remnant. 'pre-WD' indicates values just after departing from the AGB, while the last three columns correspond to the same quantities at the beginning of the WD phase (after the H-re-ignition close to the knee in the HR diagram).

Remnant mass ($M_\odot$)	$M_{env}^{pre\text{-}WD}(M_\odot)$	$M_{Buffer}^{pre\text{-}WD}(M_\odot)$	$M_H^{pre\text{-}WD}(M_\odot)$	$M_{env}(M_\odot)$	$M_{Buffer}(M_\odot)$	$M_H(M_\odot)$
0.539 46	1.07×10^{-3}	1.37×10^{-4}	6.7×10^{-4}	8.5×10^{-4}	4.38×10^{-4}	4.2×10^{-4}
0.540 06	1.67×10^{-3}	1.37×10^{-4}	1.1×10^{-3}	8.9×10^{-4}	1.00×10^{-3}	4×10^{-4}
0.540 76	2.37×10^{-3}	1.4×10^{-4}	1.64×10^{-3}	9.9×10^{-4}	1.6×10^{-3}	4.9×10^{-4}
0.541 15	2.8×10^{-3}	1.4×10^{-4}	1.94×10^{-3}	9×10^{-4}	2.06×10^{-3}	4.7×10^{-4}
0.541 48[a]	3.0×10^{-3}	1.4×10^{-4}	2.15×10^{-3}	9×10^{-4}	2.30×10^{-3}	4.5×10^{-4}

[a]This sequence did not undergo a DIN (see text for details).

shutting down winds in our reference sequence at different times immediately after the maximum of He-burning, during the final thermal pulse. Then, the remnant leaves the AGB with thicker H-rich envelopes (and slightly different final masses). As a consequence, when these remnants contract towards the WD stage, the re-ignition of H leads to thicker He-buffers. Hence, we are able to follow the cooling of WDs with different He-buffer thicknesses (see Table 1). Interestingly enough, the H-envelope mass of the WD is mostly dependent on the metallicity and not on the detailed treatment of mass loss.

As shown in Table 1 all the remnants derived from our $0.85\,M_\odot$ $Z = 0.0001$ sequence reach the WD stage with very similar H-rich envelopes (within a $\sim$10 per cent difference in mass). This is because the H-rich envelope of WDs is mostly dependent on the mass of the remnant and initial metallicity. On the other hand, remnants display significantly different He-buffers thicknesses (with differences up to a factor of 5). As a consequence of this difference, the CNO-flash develops at different points (luminosities) in the WD cooling track.

In fact, the thicker the He-buffer, the longer is the time needed for diffusion to mix enough H and C in the He-buffer and trigger the CNO-flash (see Table 2). Also, we find that in our $0.85\,M_\odot$ $Z = 0.0001$ sequence, if the He-buffer mass is $M_{Buffer} \gtrsim 2.1 \times 10^{-3}\,M_\odot$ the sequence does not experience a DIN. In Fig. 4 we show the light curves computed for these sequences. In Table 3, we show the expected abundances for major chemical elements at the surface of the star during the nova outburst. As mentioned in the previous section, the mixing of material from the He-buffer with that at the H-rich envelope by convection leads to an enhancement of the surface abundances of He and N at the expenses of the H abundance. Depending on the relative masses of the He-buffer and the H-rich envelope the outcome of such mixing gives different values of H, He and N. In fact, for those sequences with thicker He-buffers, the amount of He mixed during the CNO-flash is higher. This can be clearly appreciated from both Tables 1 and 2: the remnants that enter the WD stage with relatively thicker He-buffers are those which end with larger He-abundances after the eruption. In all the cases, however, only a

Table 2. Outburst properties of the DINs studied in this work. Unless stated otherwise, all sequences come from ZAMS progenitors with $Z = 0.0001$. Time-scales are defined as follows: cooling time at the moment of the CNO-flash (τ_1), expansion time from the maximum energy release to the giant stage at $\log T_{\rm eff} = 3.9$ (τ_2), duration of the cool ($\log T_{\rm eff} < 4$) giant stage (τ_3) and contraction time needed to reach the pre-outburst luminosity (τ_4). [a]These remnants were obtained by reducing the mass lost during the final AGB thermal pulse from that predicted by standard AGB wind prescriptions. [b]This remnant was obtained by applying an artificially high wind during the fifth thermal pulse. [c]These DINs were obtained from the $0.53946\,M_\odot$ sequence by including OV in the convective zone generated during the CNO-flash. [d]In this case the intershell composition of the remnant was modified to resemble the C- and O-rich surface abundances of PG1159 stars. IM86 indicates the sequence computed by Iben & MacDonald (IM86).

Progenitor mass	WD mass	$\log L_{\rm pre}(L_\odot)$	$\log T_{\rm eff}^{\rm pre}$	τ_1 (yr)	τ_2 (yr)	$|{\rm d}M_V/{\rm d}t|$	τ_3 (yr)	τ_4 (yr)
$0.85\,M_\odot$	$0.53946\,M_\odot$	-0.31	4.57	7.6×10^6	7.9	1.6	260	$\lesssim 1.6 \times 10^5$
$0.85\,M_\odot$	$0.54006\,M_\odot{}^a$	-0.46	4.54	1.2×10^7	10.2	1.3	–	–
$0.85\,M_\odot$	$0.54076\,M_\odot{}^a$	-0.96	4.42	4×10^7	4.9	1.6	–	–
$0.85\,M_\odot$	$0.54115\,M_\odot{}^a$	-1.19	4.37	7.7×10^7	2.7	2.4	–	–
$1\,M_\odot$	$0.55156\,M_\odot$	-0.33	4.57	6.5×10^6	3	3.3	270	9.7×10^4
$1.25\,M_\odot$	$0.59606\,M_\odot$	-0.05	4.65	3.4×10^6	4.2	2.9	216	5.5×10^4
$1.8\,M_\odot$	$0.62361\,M_\odot{}^b$	0.25	4.73	2.2×10^6	5.7	2.7	49	3.1×10^4
$1\,M_\odot$ ($Z = 0.001$)	$0.55809\,M_\odot$	-0.47	4.54	8.9×10^6	2.1	3.9	456	1.1×10^5
$0.85\,M_\odot$	$0.53946\,M_\odot$ (w/OV)^c	-0.31	4.57	7.6×10^6	0.66	6.2	1367	5.2×10^4
$0.85\,M_\odot$	$0.53946\,M_\odot$ (w/OV, CO-rich)^{c,d}	-0.03	4.63	4.1×10^6	0.42	3.1	1628	5.8×10^4
IM86 ($Z = 0.001$)	$0.6\,M_\odot$	-0.54	4.52	$\sim 10^7$	~ 7.5	–	–	–

Table 3. Outburst abundances of the DIN sequences presented in Table 2.

Progenitor mass	WD mass	H	He	C	N	O
$0.85\,M_\odot$	$0.53946\,M_\odot$	0.39	0.61	10^{-5}	2.2×10^{-4}	1.1×10^{-6}
$0.85\,M_\odot$	$0.54006\,M_\odot$	0.28	0.72	4×10^{-6}	6.1×10^{-5}	3.6×10^{-7}
$0.85\,M_\odot$	$0.54076\,M_\odot$	0.19	0.81	10^{-5}	1.4×10^{-4}	10^{-6}
$0.85\,M_\odot$	$0.54115\,M_\odot$	0.15	0.85	4×10^{-5}	3.3×10^{-4}	3.2×10^{-6}
$1\,M_\odot$	$0.55156\,M_\odot$	0.38	0.62	2×10^{-4}	4.2×10^{-3}	10^{-6}
$1.25\,M_\odot$	$0.59606\,M_\odot$	0.49	0.51	5×10^{-5}	1.3×10^{-3}	10^{-5}
$1.8\,M_\odot$	$0.62361\,M_\odot$	0.46	0.54	2×10^{-5}	4.6×10^{-3}	3×10^{-6}
$1\,M_\odot$ ($Z = 0.001$)	$0.55809\,M_\odot$	0.30	0.70	1×10^{-4}	1.9×10^{-3}	4×10^{-6}
$0.85\,M_\odot$	$0.53946\,M_\odot$ (w/OV)	0.22	0.73	6.6×10^{-3}	0.038	1.1×10^{-3}
$0.85\,M_\odot$	$0.53946\,M_\odot$ (w/OV, CO-rich)	0.23	0.62	0.033	0.081	0.033
IM86 ($Z = 0.001$)	$0.6\,M_\odot$	0.29	0.71	6.6×10^{-4}	7.5×10^{-4}	8.1×10^{-6}

mild ($\log N_{\rm H}/N_{\rm He} \approx -0.15, \ldots, 0.6$) He-enrichment is attained. It is worth mentioning that the amount of H burnt during the nova event is not significant and the star will ultimately end as an H-rich WD (DA WD).

In order to explore to what extent the mass of the remnant and its previous evolution would be relevant for the properties of DIN events, we have calculated additional sequences for different progenitor stellar masses. As in the case of our reference sequence, we have evolved these sequences from the ZAMS up to the AGB phase and tuned mass loss during the last thermal pulse in order to obtain a final thermal pulse when the H-envelope mass was already very thin (i.e. an AFTP/LTP). Again, as it happens with our reference sequence (standard AGB) winds during the AFTP/LTP erode a significant fraction of the remaining H-envelope, inhibiting an important re-ignition of the H-burning layer. Thus, WDs with very thin He-buffers are obtained. Namely, we have performed three additional cradle-to-grave sequences with $Z = 0.0001$ and ZAMS masses of $M = 1\,M_\odot$, $1.25\,M_\odot$ and $1.8\,M_\odot$. These sequences end as WDs with thin-He-buffers and masses of $0.55156\,M_\odot$ ($M_{\rm H} = 2.1 \times 10^{-4}\,M_\odot$; $M_{\rm Buffer} = 3.6 \times 10^{-3}\,M_\odot$), $0.59606\,M_\odot$ ($M_{\rm H} = 2.8 \times 10^{-4}\,M_\odot$; $M_{\rm Buffer} = 9.8 \times 10^{-5}\,M_\odot$) and $0.70492\,M_\odot$ ($M_{\rm H} = 1.8 \times 10^{-5}\,M_\odot$; $M_{\rm Buffer} = 5.9 \times 10^{-5}\,M_\odot$). While the first two sequences suffered a DIN (see Table 2 for their outburst properties), the last (more massive) one did not. In fact, in order to explore how robust this result was, we have followed a similar approach than we did with our reference sequence. By

tuning the amount of mass lost during the very last AGB phase, we obtained WDs with very similar masses but significantly different He-buffers and H-contents, namely $0.70492\,M_\odot$ ($M_{\rm H} = 1.8 \times 10^{-5}\,M_\odot$; $M_{\rm Buffer} = 5.9 \times 10^{-5}\,M_\odot$), $0.70496\,M_\odot$ ($M_{\rm H} = 4.3 \times 10^{-5}\,M_\odot$; $M_{\rm Buffer} = 5.9 \times 10^{-5}\,M_\odot$), $0.70500\,M_\odot$ ($M_{\rm H} = 7.5 \times 10^{-5}\,M_\odot$; $M_{\rm Buffer} = 8 \times 10^{-5}\,M_\odot$), $0.70540\,M_\odot$ ($M_{\rm H} = 6.2 \times 10^{-5}\,M_\odot$; $M_{\rm Buffer} = 4.8 \times 10^{-4}\,M_\odot$). We did not obtain a DIN in any of these sequences. Thus, it seems that DINs do not occur in WDs with masses significantly higher than the canonical $0.6\,M_\odot$ value. To explore further the importance of the WD mass for the development of DINs we computed additional sequences by artificially stripped mass during the fifth thermal pulse of our $1.8\,M_\odot$ sequence[3] to obtain a $0.62361\,M_\odot$ WD with a thin He-buffer ($M_{\rm H} = 2.6 \times 10^{-4}\,M_\odot$; $M_{\rm Buffer} = 7.5 \times 10^{-5}\,M_\odot$). This sequence did experience a DIN and its properties are described in Table 2.

For the sake of completeness we have also performed two additional full sequences with progenitors of $M = 1\,M_\odot$ but two different metallicities; $Z = 0.001$ and 0.01. These sequences end as WDs of $0.55809\,M_\odot$ ($M_{\rm H} = 3 \times 10^{-4}\,M_\odot$; $M_{\rm Buffer} = 2.8 \times 10^{-4}\,M_\odot$) and $0.52382\,M_\odot$ ($M_{\rm H} = 2.5 \times 10^{-4}\,M_\odot$; $M_{\rm Buffer} = 5.5 \times$

[3] Under standard AGB winds the sequence experiences 17 thermal pulses before ending as a $0.70492\,M_\odot$ WD.

$10^{-4}\,M_\odot$). The first sequence did experience a nova event (see Table 2), while the second one did not.

Although the exploration of the parameter space we have made is not completely exhaustive, we can draw some preliminary conclusions. To begin with, it seems that the occurrence of DINs is confined to low-mass, low-metallicity remnants. This is true regardless of the fact that our most massive remnant, $0.704\,92\,M_\odot$, had a very thin He-buffer ($M_{Buffer} = 5.9 \times 10^{-5}\,M_\odot$). The absence of DINs in higher mass or metallicity remnants with thin He-buffers is certainly not only because of the lower H-content that higher mass/metallicity WDs *are supposed* to have. In fact, the $0.523\,82\,M_\odot$ $Z = 0.01$ sequence does not show significant differences either in mass or in the values of M_H and M_{Buffer} from that of our reference $0.539\,46\,M_\odot$ $Z = 0.0001$ sequence. The key point that seems to prevent the DIN event in our more metallic sequence is related to the luminosity of the CO-core. In fact, despite the slightly lower mass and slightly higher carbon content, our $0.523\,82\,M_\odot$ $Z = 0.01$ sequence cools significantly faster (≈ 50 per cent at $\log T_{eff} = 4.6$) than our reference $0.539\,46\,M_\odot$ $Z = 0.0001$ sequence. Consequently, the core luminosity is roughly ≈ 50 per cent higher than that of the reference sequence. This, coupled with the fact that the CNO-burning shell is ≈ 25 per cent less luminous (at $\log T_{eff} = 4.6$) than the reference sequence case, makes CNO-burning stable (see Section 4.3) and thus no DIN develops. The faster evolution of higher metallicity warm WDs was shown in Renedo et al. (2010). It seems, then, that higher metallicity tends to prevent CNO-flashes, mostly due to a faster evolution during the warm WD stage which leads to a somewhat higher gravothermal energy release in the core. In the case of our highest mass WD ($\sim 0.705\,00\,M_\odot$), the absence of CNO-flashes is related to the low luminosity of the CNO-burning shell, which is, at most (at $\log T_{eff} \sim 4.55$), $L_{CNO} \sim L_{core}$ (see Section 4.3). Then, our numerical experiments suggest that higher metallicity or masses tend to prevent the occurrence of DIN events due to the stabilizing effect of a low L_{CNO}/L_{core} value (see Section 4.3).

It must be noted that the final masses of our WD remnants are in agreement with our present understanding of the initial–final mass relationship for low-/intermediate-mass stars (Salaris et al. 2009), and thus we expect our WD models to be physically sounding. In Fig. 7, we show the light curves and effective temperature evolution during the outburst for sequences with different progenitors, metallicities and final WD masses.
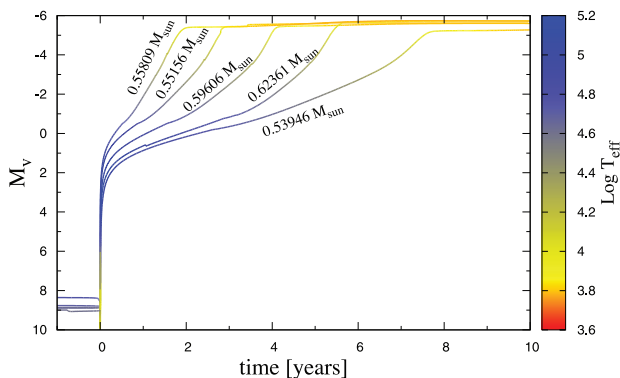

Figure 7. Predicted light curves for the DINs of remnants with different masses and descending from different progenitors (see text for details). Visual magnitudes were obtained from the predicted luminosity of the sequences and adopting the bolometric corrections derived by Flower (1996).

Finally, our simulations show that DINs have characteristic properties that make them easy to recognize. First their visual light curve displays a sudden increase, in less than a month, of 6 to 7 mag followed by slower increase in which it increases from $M_V \sim 2$ mag to its maximum of $M_V \sim -5.5$ mag in a few years – ~ 2 and ~ 10 yr depending on the remnant properties. Its brightening speed just before reaching their maximum would be of 1 to 4 mag per year. Also, as the star brightness increases the star should become cooler and yellowish (see Fig. 7). Such light curve would be probably classified as an extremely slow rising nova (IM86). Secondly, the outburst abundances (see Table 3) of all our sequences are characterized by $\log N_H/N_{He} \sim -0.15, \ldots, 0.6$ and high N abundances of 10^{-4} to 10^{-3} and C>O, by mass fraction.

4.3 The stability of CNO-burning on white dwarfs

In this section, we will try to clarify the reasons behind the instability of the CNO-burning shell by looking for a quantitative measure of the stability of H-shell burning. In this connection, we have closely followed the criterion presented by Yoon, Langer & van der Sluys (2004) and extended it to be used with mild burning shells in WDs.

Yoon et al. (2004) analysed the stability of a burning shell by investigating the reaction of its mean properties under a uniform expansion of the shell and the surrounding envelope. Specifically, they defined the burning shell (where mean quantities are calculated) as those layers where the energy generation rate is $\epsilon_{CNO} > \epsilon_{CNO\,at\,shell\,peak}/0.002$. By assuming that the inner boundary of the burning shell (r_0) remains constant, neglecting the gravitational energy release of the unperturbed model, and neglecting both the luminosity of the core ($l_0 = 0$) and its perturbation ($\delta l_0 = 0$), Yoon et al. (2004) found that the temperature perturbation $\theta = \delta T/T$ follows the equation

$$\tau_{th}\dot{\theta} = \sigma\theta, \tag{1}$$

where τ_{th} is the thermal time-scale of the shell and σ is given by

$$\sigma = \frac{\epsilon_T + \kappa_T - 4 + \dfrac{\alpha_T}{(\alpha_P\alpha_s - 1)}\left(\epsilon_\rho + \alpha_s + \kappa_\rho\right)}{1 - \nabla_{ad}\dfrac{\alpha_s\alpha_T}{(\alpha_P\alpha_s - 1)}}, \tag{2}$$

where $\epsilon_T, \epsilon_\rho, \kappa_T, \kappa_\rho$ are the logarithmic derivatives of $\epsilon(T, \rho)$ and $\kappa(T, \rho)$ while α_T, α_P are the logarithmic derivatives of $\rho(T, P)$. α_s is a parameter describing the geometrical thickness of the burning shell (see Yoon et al. 2004). Then, σ is the parameter quantifying the shell instability, so that $\sigma < 0$ ($\sigma > 0$) corresponds to stable (unstable) burning.

In our case, an important shortcoming of this approach comes from the fact that the CNO-burning shell is not clearly detached from the outer pp-burning shell. Thus, the choice of the borders of the simplified burning shell is not as easy as in usual burning shells (see Yoon et al. 2004). For the present analysis we have chosen the lower boundary of the shell as the point at which $\epsilon_{CNO} = \epsilon_{CNO\,at\,shell\,peak}/10$, which is close to the point at which the structural effects of the burning shell start to be apparent. For the outer boundary we have chosen it to be the point closest to the shell maximum at which either $\epsilon_{CNO} = \epsilon_{pp}$ or $\epsilon_{CNO} = \epsilon_{CNO\,at\,shell\,peak}/10$. The other important issue comes from the fact that the core luminosity l_0 (see Yoon et al. 2004) cannot be neglected in our case, due to the relative importance of the gravothermal energy release from the core as compared to the shell luminosity ($l_{CNO} = l_s - l_0$, where l_s stands for the luminosity at the outer boundary of the burning shell). Also, the perturbation of the luminosity at the inner boundary of the burning shell (δl_0)
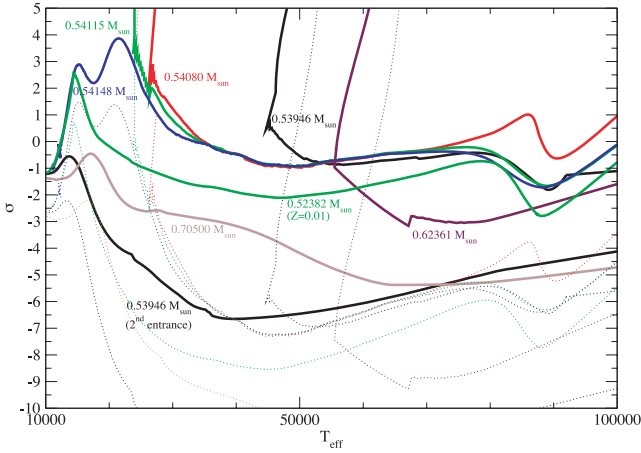
Figure 8. Evolution of the value of the stability parameter σ for selected WD sequences. Note the significantly lower σ-values of the high-mass (0.705 00 M$_\odot$) and high-metallicity (0.523 82 M$_\odot$, $Z = 0.01$) sequences which denote the stability of CNO-burning for those sequences. Also note the very low σ-value of our reference sequence during its second evolution of the WD stage.

cannot be neglected either.[4] Within the scheme presented by Yoon et al. (2004) δl_0 cannot be derived and, thus, we will consider it to be proportional to δl_s. It is clear that, for the reasons mentioned above, we cannot expect from this approach to get a quantitative prediction of the instability of the CNO-burning shell, but we will show that its qualitative description is very useful to understand the causes beneath the shell instability.

Under the assumptions and definitions mentioned above it is easy to show that the criterion of Yoon et al. (2004) is modified so that the parameter σ quantifying the shell instability is defined as

$$\sigma = \frac{\epsilon_T\,x + \kappa_T\,y - 4\,y + \dfrac{\alpha_T}{(\alpha_P\alpha_s - 1)}\left(\epsilon_\rho\,x + \alpha_s\,y + \kappa_\rho\,y\right)}{1 - \nabla_{ad}\dfrac{\alpha_s\alpha_T}{(\alpha_P\alpha_s - 1)}}. \qquad (3)$$

The main difference with the criterion presented by Yoon et al. (2004) comes from the presence of the parameters $x = (l_s - l_0)/l_s$ and $y = (\delta l_s - \delta l_0)/\delta l_s$. For the present analysis we have adopted extreme values for y; $y = 1$ [$\delta l_0 = 0$, as in Yoon et al. 2004] and $y = 2$ (i.e. $\delta l_0 = -\delta l_s$).

In all our sequences $\alpha_s < 0.16$ so the behaviour of the burning shell is not far from that of *thin* burning shells, where

$$\sigma_{thin} \sim \epsilon_T\,x + \kappa_T\,y - 4\,y + \alpha_T(\epsilon_\rho\,x + \kappa_\rho\,y). \qquad (4)$$

In the absence of a core luminosity ($x = 1$) σ_{thin}, and thus instability, is dominated by ϵ_T. However, in our sequences we find the factor x to play a very important role as its values range from $x \sim 0.5$ for the 0.539 46 M$_\odot$ sequence just before the flash to less than 0.2 for the 0.705 00 M$_\odot$ sequence at its maximum value. An exploration of our sequences shows that the term $\epsilon_T\,x$ is dominant in the behaviour of σ.

In Fig. 8, we show the evolution of the parameter σ for some selected sequences. As expected, the quantitative prediction of the instability is not reproduced. However qualitatively, Fig. 8 shows that instabilities develop during the rise in the parameter σ which is caused by the increase in ϵ_T due to the cooling of the shell. However, this increase in ϵ_T is counterbalanced by the decrease

---

[4] Note that this is also true for those cases in which $l_0 \sim 0$.

in x as a consequence of the dimming of the shell. The interplay between these two main factors is crucial for the development of the instability. Diffusion leads to an increase in the CNO-burning shell power, which increases x and might trigger the flash. If, by the time diffusion starts to change the H-content at the H-burning layers, the shell is already very dim H-burning remains stable and no DIN develops. The existence of a thicker He-buffer delays the effect of diffusion and thus, if the buffer is thick enough H-burning remains stable during the WD cooling. From Fig. 8 we can also understand why higher mass sequences ($M \sim 0.705\,00$ M$_\odot$) do not undergo DIN events despite the very thin helium buffers. The reason is that burning shells are too dim as compared with the core luminosity and, thus, very low x values render H-burning stable. In the case of the high metallicity ($Z = 0.01$) 0.523 82 M$_\odot$ sequence discussed in previous sections, its faster cooling (than our reference $Z = 0.0001$ sequences of similar mass) is tied to a higher core luminosity which makes CNO-burning stable.

Thus, our analysis suggests that CNO-flashes depend on the intensity of the CNO-burning shell (compared to the core luminosity, i.e. x) and its temperature (i.e. ϵ_T). Both factors depend on diffusion velocities, which mix H into deeper, hotter, layers increasing the CNO-burning power, and the thickness of the He-buffer which delays the contact between C and H. Finally, the relative intensity of the CNO-burning shell compared to the core luminosity depends on the mass and (progenitor) metallicity of the WD, a fact that seems to prevent DIN events in higher mass and metallicity remnants.

4.4 Effect of extramixing in the CNO-flash-driven convective zone

In the interests of completeness we have also analysed the impact of extramixing in the flash-driven convective zone. In this connection, we have recalculated the DIN event for our reference sequence including extramixing beyond convective boundaries during the flash. This was done within the picture developed by Herwig et al. (1997) of an exponentially decaying OV with $f = 0.016$ (see Herwig et al. 1997 for a definition). It is worth noting that, although the physical picture behind this prescription might not be correct, it can be considered as an effective way to include extramixing processes that take place at convective boundaries (e.g. gravity waves; see Herwig et al. 2007).

The main consequence of the inclusion of OV during the development of the CNO-flash convective zone is that H is dragged deeper into hotter regions of the star. This enhances the CNO-burning luminosity during the flash, which can be as high as $L_{CNO} \sim 10^{10}$ L$_\odot$, significantly higher than the value of $L_{CNO} \sim 10^7$ L$_\odot$ predicted by no-OV sequences. Also, due to the fact that the convective zone reaches deeper during the flash, much more material from the N-rich He-buffer (and even from the C-rich intershell) is dragged to the surface during the outburst. As a consequence the surface abundances during the outburst are significantly enhanced in He and N (see Table 3). Also, surface C and O are strongly increased to $\sim 10^{-3}$ (by mass fractions), as compared with the 10^{-5} to 10^{-6} resulting from the case when OV is neglected. It is worth mentioning that the increase in C and O would be higher if the intershell abundance of the model is richer in C and O (see Section 5.2 and Table 3). Also, as the CNO energy release is orders of magnitude higher when OV is considered, the event is more violent, reaching the giant stage in less than a year and showing a much steeper outburst light curve (see Table 2). Also, when OV is included the duration of the giant stage (τ_3, Table 2) is also enhanced, being of the order of $\sim 10^4$ yr. This is because much more H is consumed in this case and

consequently much more energy is released, allowing for a longer giant stage. Also as a consequence of this higher H-burning, the amount of H remaining in the star by the time it reenters the WD stage is about $M_H \sim 10^{-5} \, M_\odot$, six times smaller than in the no-OV case ($M_H \sim 5.7 \times 10^{-5} \, M_\odot$).[5]

4.5 Comparison with Iben & MacDonald (1986)

In this section we compare our results with those of the DIN calculated by IM86. In Table 2 we show the main characteristics of our simulations together with those extracted from IM86. An examination of IM86 results show that all the predicted quantities fall within the range predicted by our simulations. In particular, it is worth noting that the time, luminosity and temperature at which the nova takes place in the simulation of IM86 are very similar to those of our sequence of similar metallicity (although different mass). The same is true for the abundances of He and H during the outburst. In view of the many numerical and physical differences between IM86 and our simulations, we consider the similarities of both results as a strong indication for the robustness of the results and the feasibility of the scenario. In particular, we feel confident that the results presented in Tables 2 and 3 reflect the main characteristics of DIN outbursts.

Regarding the work by IM86 some comments need to be done. The authors conclude that if the He-buffer thickness is smaller than a critical value given by $M_{Buffer}^{CRIT} \sim \Delta M_H/10$, where ΔM_H stands for the increase of the H-free core during the interpulse phase on the AGB, then a DIN occurs. This conclusion has been recently used by Lawlor & MacDonald (2006) to conclude that DINs cannot occur in WDs descending from progenitors of masses lower than $3 \, M_\odot$. This result is completely at variance with the results presented in the previous sections where all DINs come from low-mass progenitors. However, it should be mentioned that the condition $M_{Buffer}^{CRIT} \sim \Delta M_H/10$ seems to be based on a single sequence, and thus it may be wrong to extrapolate it to remnants of different masses. During the present study we have not found such a 'critical value' to be fulfilled. In fact, in our $0.85 \, M_\odot$ sequences we find the frontier between the development or not of a diffusion nova to take place somewhere between our $0.541\,48 \, M_\odot$ ($M_{Buffer} = 2.3 \times 10^{-3} \, M_\odot$) and our $0.541\,48 \, M_\odot$ ($M_{Buffer} = 2.06 \times 10^{-3} \, M_\odot$) remnant. For these sequences, the increase of the H-free core between thermal pulses is $\Delta M_H = 0.0101 \, M_\odot$, very similar to the IM86 value. Then, the critical He-buffer thickness is $M_{Buffer}^{CRIT} \sim 2 \times 10^{-3} \sim \Delta M_H/5$. This is two times larger than suggested by IM86. On the other hand, for our $1.8 \, M_\odot$ progenitor we find that while our $0.6236 \, M_\odot$ ($M_{Buffer} = 7.5 \times 10^{-5} \, M_\odot$) WD remnant does experience a CNO-flash, our slightly more massive remnant of $0.6239 \, M_\odot$ ($M_{Buffer} = 3 \times 10^{-4} \, M_\odot$) does not. Then, as the increase of the H-free core for the $1.8 \, M_\odot$ sequence during the fifth thermal pulse is $\Delta M_H = 0.009$, then the critical He-buffer thickness is $M_{Buffer}^{CRIT} \sim \Delta M_H/\alpha$ with α a number between 30 and 120. Finally, let us mention that when we followed the AGB evolution of our $1.8 \, M_\odot$ sequence up to the 17th thermal pulse, the growth of the H-free core during the interpulse phases is $\Delta M_H = 0.0059 \, M_\odot$. For the WD remnants created from this progenitor, even in the case with the thinner He-buffer, $0.704\,92 \, M_\odot$ ($M_{Buffer} = 5.9 \times 10^{-5} \, M_\odot$), we did not obtain a DIN. Even though in this case $M_{Buffer} = \Delta M_H/100$, no DIN developed.

This is in line with our analysis of Section 4.3 that suggests that for these WD masses DIN events will not develop, regardless of the He-buffer mass. Then, we conclude that the previously mentioned critical He-buffer mass for the development of a DIN is misleading. As mentioned in Section 4.3 it is clear that the He-buffer thickness is not the only ingredient that determines whether a DIN will occur.

Finally, IM86 speculate[6] that DINs might be recurrent. As mentioned in the Introduction, the occurrence of recurrent DIN episodes has been invoked (D'Antona & Mazzitelli 1990) as a possible mechanism to explain the existence of DA WDs with thin H-envelopes (as those inferred by some asteroseismological studies; e.g. Castanheira & Kepler 2009). Our computation of the aftermath of the DIN shows that the star evolves much faster during its second cooling stage as a WD and, thus, diffusion has no time to significantly alter the chemical profiles of the inner regions of the WD. As a consequence, H-burning during the second WD evolution remains stable and no recurrent DIN events can develop.

5 POSSIBLE OBSERVATIONAL COUNTERPARTS

5.1 Speculations on the origin of CK Vul

In the previous sections we have presented the predictions of the DIN scenario. As these events have been suggested to look like 'very slow novae' it seems natural to compare their predictions with some of those objects. The most famous and enigmatic one is Hevelius nova CK Vul (Shara et al. 1985). Here, we will compare the predictions of the DIN with observations from CK Vul and with the predictions of the best available scenario, the VLTP (Harrison 1996; Evans et al. 2002; Hajduk et al. 2007).

5.1.1 Surface composition, H-abundance

One of the most remarkable difference between VLTP models and observations of CK Vul come from the significant H emission detected in the ejected material of CK Vul, in contrast with the extreme H-deficiency detected in the ejected material of the two bona fide VLTP objects; V4334 Sgr and V605 Aql (Hajduk et al. 2007). In this connection, the DIN scenario predicts a high H-content in the envelope during the outburst and, thus, of the ejected material (see Table 3), contrary to the predictions of the VLTP scenario (see Miller Bertolami & Althaus 2007). Also it is worth noting that the most abundant CNO element predicted by the DIN scenario is N, which is clearly detected in CK Vul surrounding material (Hajduk et al. 2007).

5.1.2 Absence of an old planetary nebula

From the low dust emission surrounding CK Vul, Hajduk et al. (2007) conclude that CK Vul must be an evolved object 10^5–10^6 yr older than the last time it experienced steady high mass loss (e.g. on the TP-AGB). This time is orders of magnitude longer than the time from the departure of the TP-AGB to a VLTP ($\sim 10^4$ yr). In fact, both V4334 Sgr and V605 Aql show old planetary nebulae surrounding the new ejected material (Kimeswenger et al. 2007). On the contrary, the DIN scenario predicts a much longer time-scale between the cessation of high mass loss and the time of the

---

[5] Note that this factor corresponds also to the difference between the duration of the giant stage in the no-OV case, $\tau_3 = 260$ yr, and the OV case $\tau_3 = 1367$ yr.

[6] Due to numerical difficulties they stopped their simulation once the star returned back to a giant configuration.

CNO-flash. As shown in Table 2, this time-scale is of the order of 10^6–10^7 yr, in closer agreement with the observations of CK Vul.

5.1.3 Ejected mass

Due to the fact that the expanding layers in a DIN episode are those above the region of the CNO-flash, DIN models have a very stringent upper limit to the mass that can be expelled during the outburst. As an example, the location of the H-flash in our reference sequence is $\lesssim 10^{-3}$ $M_\odot$ below the surface and the expanded envelope once the star is back on the AGB is of about $\sim 10^{-4}$ $M_\odot$. Thus, we can safely conclude that the ejected mass in the DIN scenario will be of $\sim 10^{-4}$ $M_\odot$ – and surely smaller than $\sim 10^{-3}$ $M_\odot$. These values are within the inferred masses for the ejected material in CK Vul, which is of 10^{-5} $M_\odot$ to 5×10^{-2} $M_\odot$ depending on the assumptions (Hajduk et al. 2007).

5.1.4 Outburst light curve

CK Vul was discovered at its maximum brightness on 1670 June 20 of as the third magnitude star. Although no description of the outburst light curve exists, Shara et al. (1985) conclude that it is very unlikely that the star was visible in the previous season. Thus, only a lower limit to the brightness speed of ~ 2 mag per year can be established. This limit is within the values predicted by the DIN scenario (see Table 2). After reaching maximum brightness it faded and recovered twice before finally disappearing from view. These fadings are remarkably similar to those observed in born-again AGB stars (V605 Aql; Duerbeck et al. 2002 and V4334 Sgr; Duerbeck et al. 2000) and RCrB stars (Clayton 1996). In fact, this particular light curve was one of the main arguments to link CK Vul to the VLTP scenario (Harrison 1996; Evans et al. 2002). RCrB-like fading are usually associated with carbon dust, so one should wonder if such fading episodes could take place in atmospheres which are not C-rich, as those predicted by our DIN simulations (see Table 2). In this connection, we find it suggestive that there is one 'Hot RCrB', MV Sgr (De Marco et al. 2002), which has a carbon and nitrogen composition very similar (C $\sim 5 \times 10^{-4}$ and N $\sim 9 \times 10^{-4}$) to those predicted by the DIN scenario (N > C > O and N $\sim 10^{-3}$ to 10^{-4}; see Table 3), although MV Sgr shows a much stronger He-enrichment. We consider that MV Sgr suggests that DIN events might also display the fadings observed in RCrB like light curves, although we consider this just a speculation and should be analysed in detail. From these considerations we conclude that our present understanding of the DIN scenario is not in contradiction with CK Vul eruption light curve.

5.1.5 Maximum brightness

The maximum brightness is the main discrepancy between observations and models (both for DIN and for VLTP models). While observations of CK Vul suggest at the preferred distance $M_V^{\text{CKVul}} \sim -8$, DIN models predict significantly lower values of $M_V^{\text{DIN}} \sim -5.5$. It is worth noting, however, that this is even worst for VLTP models, in which fast-VLTP sequences predict $M_V^{\text{VLTP}} \sim -4$ (according to the predicted luminosities in Miller Bertolami & Althaus 2007).

5.1.6 Actual luminosity of CK Vul

One of the main discrepancies between inferences from CK Vul and both DIN and VLTP scenarios comes from the radio emission. In fact, from the radio emission detected by Hajduk et al. (2007) these authors derive a very low luminosity of $\sim L_\odot$ for the ionizing object. This is done by considering that hydrogen is ionized by the photons emitted by the central object above the Lyman limit. Neither the DIN nor VLTP events can account such very low luminosities only 330 yr after the outburst. However, it is worth noting that such very low luminosity is derived from the assumption that the temperature of the central object is close to the effective temperature at which the number of ionizing photons is maximum. From the data presented by Hajduk et al. (2007) and adopting the expression from Wilcots (1994),

$$F_c = 1.761 \times 10^{48} \times a(\nu, T_e) \times \nu^{0.1} \times T_e^{-0.45} \times S \times D^2, \qquad (5)$$

we derive that the number of ionizing photons is $N_\gamma \sim 4 \times 10^{43}$ s^{-1}. As the number of ionizing photons is steeply dependent on the effective temperature of the star, such a number of photons can also be attained by a star of $T_{\text{eff}} \sim 10\,000$ K and $L \sim 10\,000$ L$_\odot$. These values put the central object back in the AGB region of the HR diagram. Hence we are tempted to speculate that the radio emission could be compatible with an object reheating back from the second stage in the AGB and, thus, compatible with both VLTP and DIN scenarios. However, increasing the luminosity of the star should increase the IR-flux from the obscuring material (Evans et al. 2002). One may thus wonder if the IR-flux would be much higher than the observational limits (e.g. $S_{12} \sim$ mJy; Hajduk et al. 2007). Some rough numbers show that this would be strongly dependent on the geometrical and physical assumptions on the obscuring material. For example, if we assume the star being obscured by a circumstellar shell located at $r \sim 30$ au (and assumed to behave as a blackbody), we obtain a shell temperature of $T_{\text{dust}} \approx 720$ K and a flux of $S_{12} \sim 1000$ Jy, several orders of magnitude above the observational upper limit (Hajduk et al. 2007). On the contrary if the star is obscured by the presence of a pre-existing edge-on disc ($r_{\text{inner}} = 1$ au, $r_{\text{outer}} = 60$ au and height $h = 1$ au), as suggested by the ejection almost perpendicular to the line of sight, then the IR-flux would be much lower. Indeed, by assuming a classical temperature profile ($T \propto r^{-3/4}$; Natta 1993) and a blackbody behaviour we (roughly) estimate $S_{12} \sim 25$ mJy, much closer to the observational constraints (Hajduk et al. 2007).

We conclude that if CK Vul is actually obscured by a thick disc, the radio emission could be explained by a cool reborn giant star ($T_{\text{eff}} \sim 10\,000$ K and $L \sim 10\,000$ L$_\odot$) without a strong IR emission. This would help to reconcile the predictions of both VLTP and DIN scenarios with the observed properties of CK Vul. Then, a detailed modelling of the dust surrounding CK Vul seems to be the key in order to reject a possible luminous cool central star as the present state for CK Vul.

5.2 Possible connection with PB8

As mentioned in Section 4.4, the inclusion of extramixing processes at the boundaries of the CNO-flash-driven convective zone leads to outburst abundances rich in He, H and N (see Table 3). Also, the inclusion of extramixing processes leads to a more violent flash and to an increase in the time spent as a giant (τ_3; see Table 2) after the DIN event. During this short giant stage the reactivation of AGB winds is expected. Depending on the amount of mass lost during this stage, it could be possible that the new ejected material might form a new young planetary nebula once the star begins to contract and heat towards the second WD phase. Such a young planetary nebula would show very low dynamical ages and, together with its central star, a very atypical He-, H- and N-rich composition. PB8 has

been recently shown to have (qualitatively) similar characteristics (Todt et al. 2010; García-Rojas, Peña & Peimbert 2009), namely low dynamical age of a few thousand years and an He-, H- and N-rich composition. Specifically, the central star of PB8 has been proposed as the prototype of [WN/WC], a new class of CSPN. In particular, the surface abundances of PB8-CSPN have been derived, by Todt et al. (2010), to be [H/He/C/N/O] = [40/55/1.3/2/1.3]. These abundances can be accounted by our DIN sequences that include extramixing processes at convective boundaries (see Table 3). Indeed, as mentioned in Section 4.4, when OV is included at the CNO-flash convective zone, convection drags material from deeper layers of the WD, reaching the upper layers of the C-rich intershell. Thus, the C and O surface abundances after a DIN event will be strongly dependent on the intershell composition of the star when departing from the AGB. In fact, if intershell abundances are assumed to be similar to those of PG1159 stars (see Werner & Herwig 2006), much higher C and O abundances are obtained after a recalculation of the DIN event (see Table 3). In fact, the abundances obtained in this case are in good qualitative agreement with those derived by Todt et al. (2010) for PB8-CSPN (i.e. He $\gtrsim$ H > N $\gtrsim$ C ~ O). Also, the dynamical age derived by Todt et al. (2010), $\tau = 2600$ yr, is qualitatively similar to the giant phase duration of this sequence ($\tau_3 \sim$ 1600 yr). Taking into account that our simulations correspond to a single, arbitrarily chosen sequence, we find the similarities with the observed properties of PB8 to be remarkable. Further exploration of this possible explanation for PB8 seems natural.

6 FINAL REMARKS

We have performed a detailed exploration of the DIN scenario originally proposed by IM86. Our calculations represent a significant improvement in our understanding of CNO-flashes in warm WDs.

Our main results can be summarized as follows.

(i) We have identified a definite scenario leading to the formation of DA WDs with thin He-buffers. Such WDs are naturally formed in low-mass stars that do not experience third dredge up during the TP-AGB, and suffer from either an AFTP or a LTP.

(ii) We have explored the parameter space of the DIN scenario and shown that there is a range of values of $M_\star$, Z_{ZAMS} and He-buffer masses for which DIN occur in physically sound WD models. Our results suggest that DINs take place in WDs with $M_\star \lesssim 0.6$ and $Z_{ZAMS} \lesssim 0.001$ and thin He-buffers – as those provided by the scenario described above.

(iii) Our simulations provide a very detailed description of the events before, during and after the DIN event. In particular, our results show that DIN events are not recurrent as previously speculated. Thus, DINs do not form H-deficient WDs, or DA WDs with thin H-envelopes.

(iv) We have qualitatively described the mechanism by which the CNO-shell becomes unstable. Our analysis shows that the occurrence of CNO-flashes depends strongly on the intensity of the CNO-burning shell (as compared to the core luminosity), and its temperature. This seems to be in agreement with the fact that only our sequences with $M_\star \lesssim 0.6$ and $Z_{ZAMS} \lesssim 0.001$ and thin He-buffers experienced DIN events.

(v) Regarding the criterion presented by IM86 for the occurrence of DIN events, we find that such criterion is misleading as the He-buffer mass is not the only parameter that determines whether a DIN event will take place or not. In particular, for more massive remnants our simulations do not predict DIN for any possible He-buffer masses.

(vi) Our simulations provide a very detailed description of the expected surface abundances and light curves during the outbursts. In particular, we find that typical light curves display a maximum of $M_V \sim -5.5$, a brightness speed of a few magnitudes per year, and a mild He- and N-enrichment; with $N \sim 10^{-4}$ to 10^{-3} by mass fraction and $\log N_H/N_{He} \sim -0.15, \ldots, 0.6$. Also, in all our sequences we find surfaces abundances with N>C>O by mass fraction.

(vii) We find that the inclusion of extramixing events at the boundaries of the CNO-flash-driven convective zone leads to higher He, N, C and O abundances than in the case in which no extramixing is considered. Relative surface CNO abundances in these cases are N > C $\gtrsim$ O (by mass fractions), although the precise values will be strongly dependent on the C and O composition of the He-, C- and O-rich intershell.

(viii) Finally, with the aid of our numerical simulations, we have discussed the possibility that Hevelius nova CK Vul and PB8-CSPN could be observational counterparts of DIN events.

For CK Vul we find that despite discrepancies with observations the DIN scenario offers a possible explanation for CK Vul which is as good as the best available explanation to date (the VLTP scenario). In particular, the DIN scenario can easily explain the absence of and old planetary nebulae surrounding CK Vul and the presence of H in the ejected material, which cannot be understood easily within the VLTP scenario. Moreover, we suggest that the radio and IR emission from CK Vul (Hajduk et al. 2007) could be explained if the star is assumed to be in its giant stage and surrounded by a pre-existing dust disc. Such reinterpretation of the observations would reconcile them with both the VLTP and DIN scenarios. A further exploration of this possibility seems desirable.

Regarding PB8, our simulations show that the atypical abundances observed in PB8 (Todt et al. 2010) and the low dynamical age of its nebula (García-Rojas et al. 2009) could be qualitatively understood within the DIN scenario if extramixing is allowed at the boundaries of the CNO-flash convective zone.

REFERENCES

Althaus L. G., Serenelli A. M., Córsico A. H., Montgomery M. H., 2003, A&A, 404, 593
Althaus L. G., Serenelli A. M., Panei J. A., Córsico A. H., García-Berro E., Scóccola C. G., 2005, A&A, 435, 631
Althaus L. G., Córsico A. H., Isern J., García-Berro E., 2010a, A&AR, 18, 471
Althaus L. G., García-Berro E., Renedo I., Isern J., Córsico A. H., Rohrmann R. D., 2010b, ApJ, 719, 612
Burgers J. M., 1969, Flow Equations for Composite Gases. Academic Press, New York
Castanheira B. G., Kepler S. O., 2009, MNRAS, 396, 1709
Clayton G. C., 1996, PASP, 108, 225
D'Antona F., Mazzitelli I., 1990, ARA&A, 28, 139
De Marco O., Clayton G. C., Herwig F., Pollacco D. L., Clark J. S., Kilkenny D., 2002, AJ, 123, 3387
Duerbeck H. W. et al., 2000, AJ, 119, 2360
Duerbeck H. W., Hazen M. L., Misch A. A., Seitter W. C., 2002, Ap&SS, 279, 183

Evans A., van Loon J. T., Zijlstra A. A., Pollacco D., Smalley B., Tyne V. H., Eyres S. P. S., 2002, MNRAS, 332, L35

Flower P. J., 1996, ApJ, 469, 355

García-Berro E. et al., 2010, Nat, 465, 194

García-Rojas J., Peña M., Peimbert A., 2009, A&A, 496, 139

Guandalini R., Busso M., Ciprini S., Silvestro G., Persi P., 2006, A&A, 445, 1069

Hajduk M. et al., 2007, MNRAS, 378, 1298

Hansen B., 2004, Phys. Rep., 399, 1

Harrison T. E., 1996, PASP, 108, 1112

Herwig F., Bloecker T., Schoenberner D., El Eid M., 1997, A&A, 324, L81

Herwig F., Freytag B., Fuchs T., Hansen J. P., Hueckstaedt R. M., Porter D. H., Timmes F. X., Woodward P. R., 2007, in Kerschbaum F., Charbonnel C., Wing R. F., eds, ASP Conf. Ser. Vol. 378. Why Galaxies Care About AGB Stars: Their Importance as Actors and Probes. Astron. Soc. Pac., San Francisco, p. 43

Iben I., Jr, 1984, ApJ, 277, 333

Iben I., Jr, 1995, Phys. Rep., 250, 2

Iben I., Jr, MacDonald J., 1985, ApJ, 296, 540

Iben I., Jr, MacDonald J., 1986, ApJ, 301, 164 (IM86)

Kalirai J. S., Hansen B. M. S., Kelson D. D., Reitzel D. B., Rich R. M., Richer H. B., 2008, ApJ, 676, 594

Karakas A., 2003, Asymptotic Giant Branch Stars: Their Influence on Binary Systems and the Interstellar Medium. Monash University, Melbourne

Karakas A. I., Lattanzio J. C., Pols O. R., 2002, Publ. Astron. Soc. Aust., 19, 515

Kato T., 2003, A&A, 399, 695

Kimeswenger S., Zijlstra A. A., van Hoof P. A. M., Hajduk M., Lechner M. F. M., van de Steene G. C., Gesicki K., 2007, in Corradi L., Manchado A., Soker N., eds, Asymmetrical Planetary Nebulae IV, Symmetry and Asymmetry in 'born again' Planetary Nebulae, IAC electronic publication

Koester D., Chanmugam G., 1990, Rep. Prog. Phys., 53, 837

Lawlor T. M., MacDonald J., 2006, MNRAS, 371, 263

Mazzitelli I., D'Antona F., 1986, ApJ, 308, 706

Miller Bertolami M. M., Althaus L. G., 2006, A&A, 454, 845

Miller Bertolami M. M., Althaus L. G., 2007, MNRAS, 380, 763

Miller Bertolami M. M., Althaus L. G., Serenelli A. M., Panei J. A., 2006, A&A, 449, 313

Miller Bertolami M. M., Althaus L. G., Unglaub K., Weiss A., 2008, A&A, 491, 253

Natta A., 1993, ApJ, 412, 761

Renedo I., Althaus L. G., Miller Bertolami M. M., Romero A. D., Córsico A. H., Rohrmann R. D., García-Berro E., 2010, ApJ, 717, 183

Salaris M., Cassisi S., 2005, Evolution of Stars and Stellar Populations. Wiley, Hoboken, NJ

Salaris M., Serenelli A., Weiss A., Miller Bertolami M., 2009, ApJ, 692, 1013

Schröder K., Cuntz M., 2005, ApJ, 630, L73

Shara M. M., Moffat A. F. J., 1982, ApJ, 258, L41

Shara M. M., Moffat A. F. J., Webbink R. F., 1985, ApJ, 294, 271

Todt H., Peña M., Hamann W., Gräfener G., 2010, A&A, 515, A83

Trimble V., 2000, PASP, 112, 1

Vassiliadis E., Wood P. R., 1993, ApJ, 413, 641

Werner K., Herwig F., 2006, PASP, 118, 183

Wilcots E. M., 1994, AJ, 107, 1338

Yoon S., Langer N., van der Sluys M., 2004, A&A, 425, 207

This paper has been typeset from a TEX/LATEX file prepared by the author.